Design of a Wearable Lower-Limb Assisted Walking Device Control System Based on STM32

Ran Xu, Xu Wang*

Department of Intelligent Manufacturing Engineering, University of Electronic Science and Technology of China, Chengdu Campus; Chengdu 611731, China

Received: June 3, 2026

Revised: June 4, 2026

Accepted: June 5, 2026

Published online: July 2, 2026

To appear in: *International Journal of Advanced AI Applications,* Vol. 2, No. 7 (August 2026)

* Corresponding Author: Xu Wang (34106831@qq.com)

Abstract. With the intensification of population aging, the number of patients with lower-limb motor dysfunction continues to increase, and existing assisted walking devices suffer from insufficient intelligence. To address this, this paper designs a wearable lower-limb assisted walking device control system based on the STM32F103C8T6 microcontroller. The system employs MPU6050 inertial measurement units and rotary potentiometers to acquire hip and knee joint angles, combined with plantar pressure sensors for gait phase recognition. Four DC motors are driven by TB6612FNG drivers to output assistive torque. Wi-Fi communication enables data exchange with a host computer, while an OLED display, buttons, and a buzzer constitute the human-machine interaction layer. Experimental results demonstrate that the system achieves a gait recognition accuracy of 93.6%, motor response time of 22 ms, joint angle error of ±1.3°, and a battery life of approximately 1.3 hours. The system exhibits good real-time performance and reliability, and can effectively assist patients with lower-limb impairment in daily walking, demonstrating considerable potential for wider application.

Keywords: *STM32; Wearable Lower-Limb Rehabilitation Assisted Walking Device; Control System; Motor Drive; Gait Recognition; Embedded System*

1. Introduction

With the deepening of societal intelligence and the intensification of an aging population, the market demand for intelligent elderly care and rehabilitation equipment has become increasingly urgent and pronounced. In particular, advanced assisted walking devices designed specifically for the elderly can effectively enhance walking balance and significantly reduce the risk of falls. Therefore, the development of high-performance assisted walking devices for seniors not only holds substantial market potential but also offers significant economic value and societal benefits in promoting independence and improving quality of life.

In recent years, domestic universities and enterprises have significantly intensified their research and development efforts focused on advanced assisted walking devices, achieving notable results in enhancing mobility solutions. For example, in 2023, Yafen Xu, Hua Zhang, and Linfeng Yu from Guangdong University of Science and Technology designed an innovative intelligent assisted walker that features position monitoring, emergency braking, and robust wireless communication functions, which collectively achieve satisfactory mobility assistance for users [1]. In 2024, Jialiang Tan from Hefei University of Technology developed a state-of-the-art lower-limb assistive exoskeleton capable of energy recovery by integrating motor drive, metamorphic, and variable stiffness principles, demonstrating effective walking assistance tailored to the needs of individuals with mobility impairments [2]. Furthermore, in 2025, Tangjian Zeng from the University of Electronic Science and Technology of China developed a sophisticated two-degree-of-freedom hip joint exoskeleton mechanism that, while assisting elderly individuals in walking, effectively reduced human-robot interaction forces and significantly improved overall user comfort during operation [3]. The above research results indicate that developing a functionally and structurally well-designed wearable lower-limb assisted walking device requires comprehensive consideration of the user's kinematic characteristics, ergonomic design principles, and intelligent control algorithms. Based on existing research findings, this paper proposes an innovative wearable lower-limb assisted walking device control system based on the STM32F103C8T6 microcontroller, aiming to achieve real-time gait detection, adaptive motor assistance, and efficient wireless data communication for enhanced user experience.

2. System Architecture

Based on the unique walking characteristics observed in elderly individuals, we propose several essential functions crucial for the design of a lower-limb assisted walking device. These functions encompass gait detection, motor assistance, human-machine interaction, safety protection, and data communication. Each of these functions is specifically designed to enhance mobility and improve the overall user experience for elderly users. Correspondingly, we have identified specific modules that align with these functions, as detailed in Table 1. This comprehensive approach aims to provide effective and personalized support tailored to the unique needs of elderly users, ultimately promoting their independence and quality of life.

Table 1. Functions and corresponding modules.

Function	Gait Detection	Motor Assistance	Human-Machine Interaction	Data Communication	Safety Protection	Power Management
Module	Sensor perception layer: MPU6050 IMU (x2), rotary potentiometers (hip/knee x2 each), plantar pressure sensors (x8)	Drive actuation layer: TB6612FNG motor driver modules (x2), DC geared motors (hip x2, knee x2)	HMI system: 0.96-inch OLED display, buttons x3, buzzer	Communication system: Wi-Fi module (ESP-01S)	Joint angle soft limiting, motor overcurrent detection, low voltage alarm	Power system: 11.1 V Li-ion battery, LM2596 buck (→5 V), AMS1117-3.3 (digital 3.3 V), TPS73633 (analog 3.3 V)

Based on the corresponding modules shown in Table 1, the overall system architecture is illustrated in Figure 1.

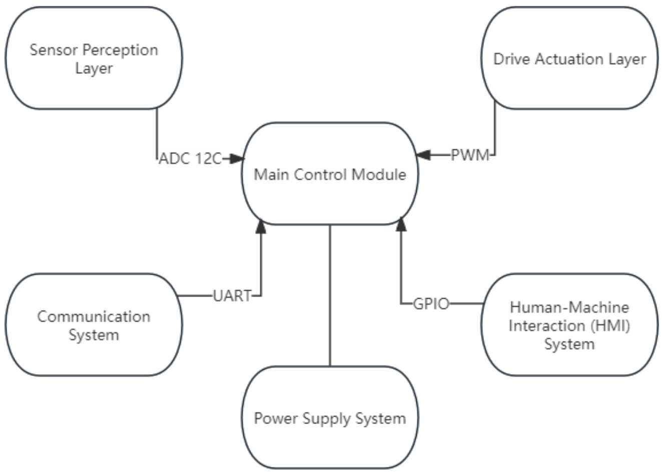

Figure 1. Overall system architecture.

3. Hardware Design

The hardware design of this system is centered on the STM32F103C8T6 microcontroller, constructing a complete control hardware platform comprising five functional modules: main control, drive, sensor, communication, and power supply. The main control chip is based on the ARM Cortex-M3 core with a clock frequency of 72 MHz, integrating on-chip peripherals including multiple ADC channels, I2C, USART, and PWM timers. The minimum system includes power decoupling, an 8 MHz crystal oscillator clock, a reset circuit, BOOT startup configuration, and an SWD debugging interface. The drive module employs two TB6612FNG dual H-bridge chips, receiving 20 kHz PWM signals from the main controller to independently control four DC geared motors for the left/right hip and knee joints. Motor forward/reverse rotation and braking are achieved through GPIO level combinations. The sensor layer consists of MPU6050 six-axis IMUs, rotary potentiometers, and plantar pressure sensors, with the IMUs mounted on the left and right thigh segments respectively.

3.1. Main Controller Design

This system utilizes the STM32F103C8T6 microcontroller from STMicroelectronics as the central control chip. The STM32F103C8T6 is built on the ARM Cortex-M3 core, boasting a clock frequency of 72 MHz. It features 64 KB of Flash memory and 20 KB of SRAM, alongside a rich array of on-chip peripheral resources. These include 7 channels of 12-bit ADC capable of achieving an impressive sampling rate of up to 1 MHz, 3 USARTs, 2 I2C interfaces, 2 SPIs, and 4 general-purpose timers that support PWM output. Moreover, it offers up to 37 GPIO pins for versatile connectivity options. This chip operates efficiently within a voltage range of 2.0–3.6 V and has an operating current of approximately 36 mA during full-speed operation at 72 MHz. Importantly, it supports multiple low-power modes, such as Sleep, Stop, and Standby, making it exceptionally suitable for meeting the stringent power and size requirements commonly found in wearable devices. Its compact design and high performance contribute significantly to innovative applications in this field.

The minimum system circuit for the STM32F103C8T6 microcontroller consists of several essential components designed to ensure proper operation and functionality:

(1) Power Decoupling: A 100 nF ceramic capacitor and a 10 μF tantalum capacitor is connected in parallel between VDD and GND. This configuration effectively suppresses power supply noise, providing stable voltage levels during operation;

(2) Clock Source: An external 8 MHz passive crystal oscillator is utilized, paired with 22 pF load capacitors (C1 and C2). This setup, along with the internal PLL (Phase-Locked Loop), multiplies the main frequency to achieve an impressive speed of 72 MHz;

(3) Reset Circuit: The NRST pin is connected to ground through a 100 nF capacitor, featuring an external button that allows for manual resetting of the microcontroller when necessary;

(4) BOOT Configuration: Both BOOT0 and BOOT1 pins are grounded (connected to GND), ensuring that the system boots from the Flash memory, allowing the firmware to run correctly after reset;

(5) SWD Debugging Interface: The SWDIO, SWDCLK, GND, and 3.3 V signals are made accessible for use with the ST-Link/V2 programmer, enabling seamless downloading and debugging of the firmware for this microcontroller.

The STM32F103C8T6 minimum system is shown in Figure 2, illustrating the arrangement and connection of these critical components to facilitate effective operation.

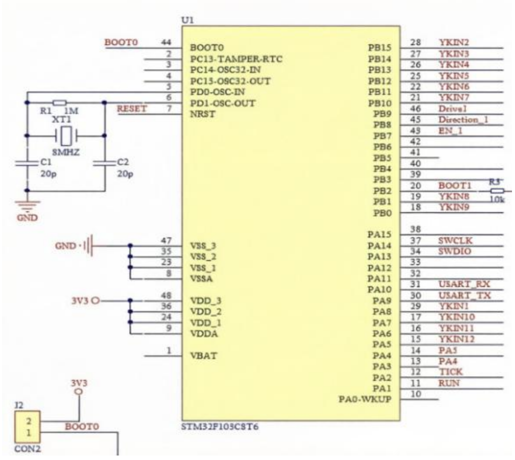

Figure 2. STM32F103C8T6 minimum system diagram.

3.2. Driver Module Design

The system is designed to effectively drive four DC geared motors, which are designated for the left and right hip joints as well as the left and right knee joints. To accomplish this task, two TB6612FNG dual H-bridge motor driver chips are employed in the setup. Each channel of the TB6612FNG provides a maximum output current of 1.2 A, with a peak capability of 3.2 A, ensuring robust performance during operation. The drive voltage range spans from 2.5 to 13.5 V, making it versatile for various applications. Additionally, it features built-in protection functions that safeguard against over-temperature, over-current, and under-voltage conditions. Importantly, the TB6612FNG is directly compatible with the STM32's 3.3 V logic level, eliminating the need for any additional level shifting components. This integration simplifies the design and enhances reliability in motor control tasks.

The driver module circuit connections are as follows:

(1) PWMA/PWMB are connected to TIM3_CH1/TIM3_CH2 (PA6/PA7) of the STM32 respectively, with the STM32 outputting 20 kHz PWM signals to control motor speed;

(2) AIN1/AIN2 and BIN1/BIN2 are connected to STM32 GPIO pins, controlling forward rotation, reverse rotation, or braking through high/low level combinations;

(3) The STBY (standby control) pin is connected to 3.3 V via a 10 kΩ pull-up resistor, enabling the chip during normal operation;

(4) The motor power supply VVM is connected to the LM2596 step-down 5 V output (maximum 12 V supply supported);

(5) A 100 μF electrolytic capacitor and a 100 nF ceramic capacitor are connected in parallel

between VM and GND to suppress back-EMF spikes. The second TB6612FNG has an identical circuit structure, controlling the right-side hip and knee joint motors respectively. The driver module circuit is shown in Figure 3.

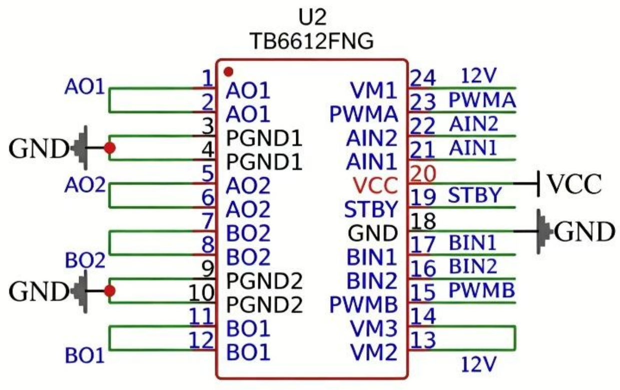

Figure 3. Driver module circuit diagram.

3.3. Sensor Module Design

The sensor perception layer of the system consists of three parts: attitude sensors, joint angle sensors, and plantar pressure sensors, which collaboratively accomplish gait phase recognition and joint state estimation.

(1) The MPU6050 attitude sensors are strategically installed on both the left and right thigh segments, providing crucial data for motion analysis. Each MPU6050 six-axis IMU module features an integrated three-axis accelerometer with a range of ±8 g and a three-axis gyroscope capable of measuring rotational speeds up to ±1000°/s. These sensors communicate seamlessly with the STM32 microcontroller via the I2C bus operating at a fast mode speed of 400 kHz. To differentiate between the left and right legs, the I2C addresses are configured to 0x68 when the AD0 pin is grounded, and 0x69 when the AD0 pin is pulled high. Furthermore, the INT interrupt pin of the MPU6050 is connected to the STM32's EXTI, enabling a trigger frequency of 100 Hz to ensure real-time gait data acquisition and processing. It's important to note that the SDA and SCL lines each require the addition of a 4.7 kΩ pull-up resistor to the 3.3 V power supply to function correctly. This setup ensures reliable communication and accurate sensor readings during operation.

(2) Joint angle potentiometers: A precision rotary potentiometer, with a resistance of 5 kΩ, is strategically installed at each hip and knee joint, resulting in a total of four analog signal channels for precise angle measurement. The two terminals of the potentiometer are connected to a stable 3.3 V supply and ground (GND), allowing the wiper to output an analog voltage range of 0–3.3 V. This output is then linked to the STM32 ADC input pins (PA0–PA3) through

a current-limiting resistor of 10 kΩ, ensuring proper signal integrity. The ADC features a sampling resolution of 12 bits, offering a quantization accuracy of approximately 0.008°. To enhance performance, a 100 nF filtering capacitor is connected in parallel between the wiper and GND, effectively suppressing high-frequency interference that can be generated during movement. This setup ensures reliable and accurate readings of joint angles for further analysis and application.

(3) Plantar pressure sensors play a vital role in gait analysis and assistive technology. In this setup, four thin-film pressure sensors (FSR402) are strategically installed on the sole of each foot, resulting in a total of eight analog signal channels designed to capture critical data. These signals are acquired using I2C multi-channel ADC expansion chips, specifically the ADS1115 model, which features four channels and offers 16-bit resolution for enhanced accuracy. The I2C addresses for the two ADS1115 chips are configured to 0x48 and 0x49 respectively, allowing seamless communication and data acquisition. This plantar pressure data is essential for determining the transition between the stance phase and the swing phase of walking, thereby enabling precise timing control for assistive devices. A visual representation of the sensor module circuit can be seen in Figure 4, illustrating the complex interactions involved in this innovative system.

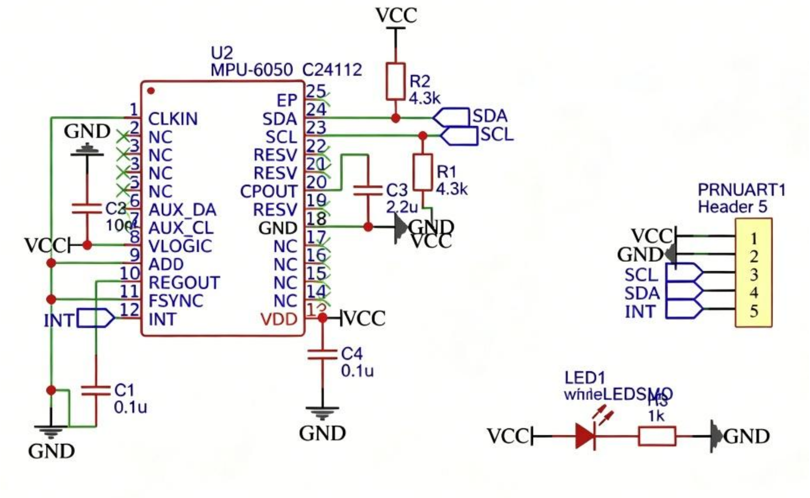

Figure 4. Sensor module circuit diagram.

3.4. Power and Communication Module Design

The system is powered by an 11.1 V (3S) lithium battery with a capacity of 2200 mAh, which undergoes a sophisticated three-stage voltage conversion to provide stable operating voltages for each subsystem.

(1) LM2596 adjustable step-down module: reduces 11.1 V to 5 V, with a maximum output

current of 3 A, supplying power to the TB6612FNG motor drivers and 5 V peripherals, with a conversion efficiency of approximately 78%;

(2) AMS1117-3.3 linear regulator: steps down 5 V to 3.3 V, with a maximum output of 200 mA, powering the STM32 main controller, Bluetooth module, OLED display, and other digital devices;

(3) TPS73633 low-noise LDO: independently generates a 3.3 V analog supply from 5 V, with a ripple voltage below 30 μV, dedicated to powering the MPU6050, potentiometers, and ADC reference voltage, implementing a single-point connection between the digital ground and analog ground to significantly reduce ADC sampling noise.

The communication module adopts the Espressif ESP-01S Wi-Fi module (ESP8266 chip), connected to the STM32 via USART1 (PA9/PA10, baud rate 115200 bps), and configured as a TCP Server using AT commands to achieve bidirectional wireless communication with a PC host computer. The ESP-01S operates at 3.3 V, conforms to the IEEE 802.11 b/g/n Wi-Fi standard, and provides an effective indoor communication range of up to 50 m, with a transmission rate significantly higher than Bluetooth BLE. It can upload gait data, motor current, joint angles, and other information in real time, while receiving parameter adjustment commands (such as assistance level, mode switching) from the host computer. To meet the peak current requirement of approximately 300 mA for the ESP-01S, the communication module is independently powered by a dedicated XC6206-3.3 V LDO regulator. The power and communication module circuit is shown in Figure 5.

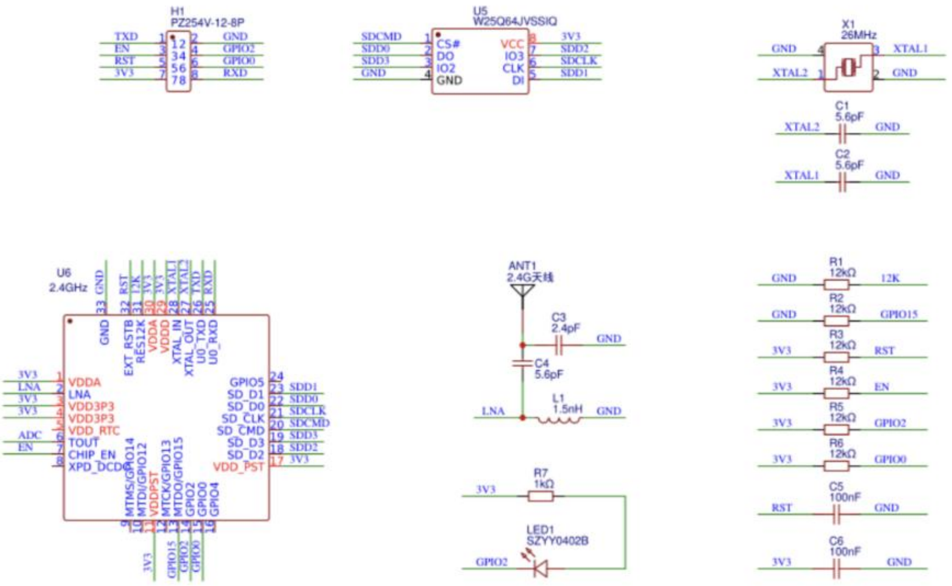

Figure 5. Sensor module circuit diagram.

4. Software Design

The system software is meticulously developed using the Keil MDK 5 environment and is implemented with the STM32 Standard Peripheral Library (SPL). The program structure adopts a well-defined foreground-background architecture: the main loop, functioning as the background, executes various gait algorithms and motor control tasks, while interrupt service routines, acting as the foreground, efficiently handle data acquisition and communication processing. This design ensures both real-time performance and enhanced code maintainability. Furthermore, the software is thoughtfully divided into six major modules for better organization: initialization, sensor driver, gait recognition, motor control, human-machine interaction, and communication. This modular approach facilitates easier troubleshooting and future enhancements.

4.1. Overall Program Design

After power-on, the system first executes the initialization sequence: configure the system clock (HSE+PLL → 72 MHz), initialize GPIO directions, configure the ADC (12-bit, continuous conversion mode), configure I2C1 (400 kHz) for MPU6050 and ADS1115 communication, configure TIM3 (20 kHz PWM output) for motor speed control, configure USART1 (115200 bps) for Wi-Fi (ESP-01S) communication (sending AT commands after power-on to initialize the module and connect to the local network), and initialize the OLED display.

The main control loop operates on a 10 ms cycle, sequentially executing the following essential steps:

(1) Read data from the MPU6050 sensor and fuse the accelerometer and gyroscope measurements through a complementary filter with a weight ($\alpha = 0.98$) to accurately calculate the trunk inclination angle;

(2) Read the ADC values from the four potentiometer channels and convert these readings into the respective hip and knee joint angles for further processing;

(3) Read the plantar pressure data using the ADS1115 to determine the current gait phase, distinguishing between the stance phase and the swing phase effectively;

(4) Based on the determined gait phase and the calculated joint angles, look up the assistive torque required for the corresponding joint in a predefined lookup table; convert this torque value into a PWM duty cycle, and then output it to the TB6612FNG motor driver;

(5) Check the status of the buttons and update the OLED display accordingly, showing

relevant information such as joint angles, the current gait phase, and the battery level to the user;

(6) Package the processed sensor data and upload it to the host computer via Wi-Fi for further analysis and logging. The overall system operation flow is visually represented in Figure 6.

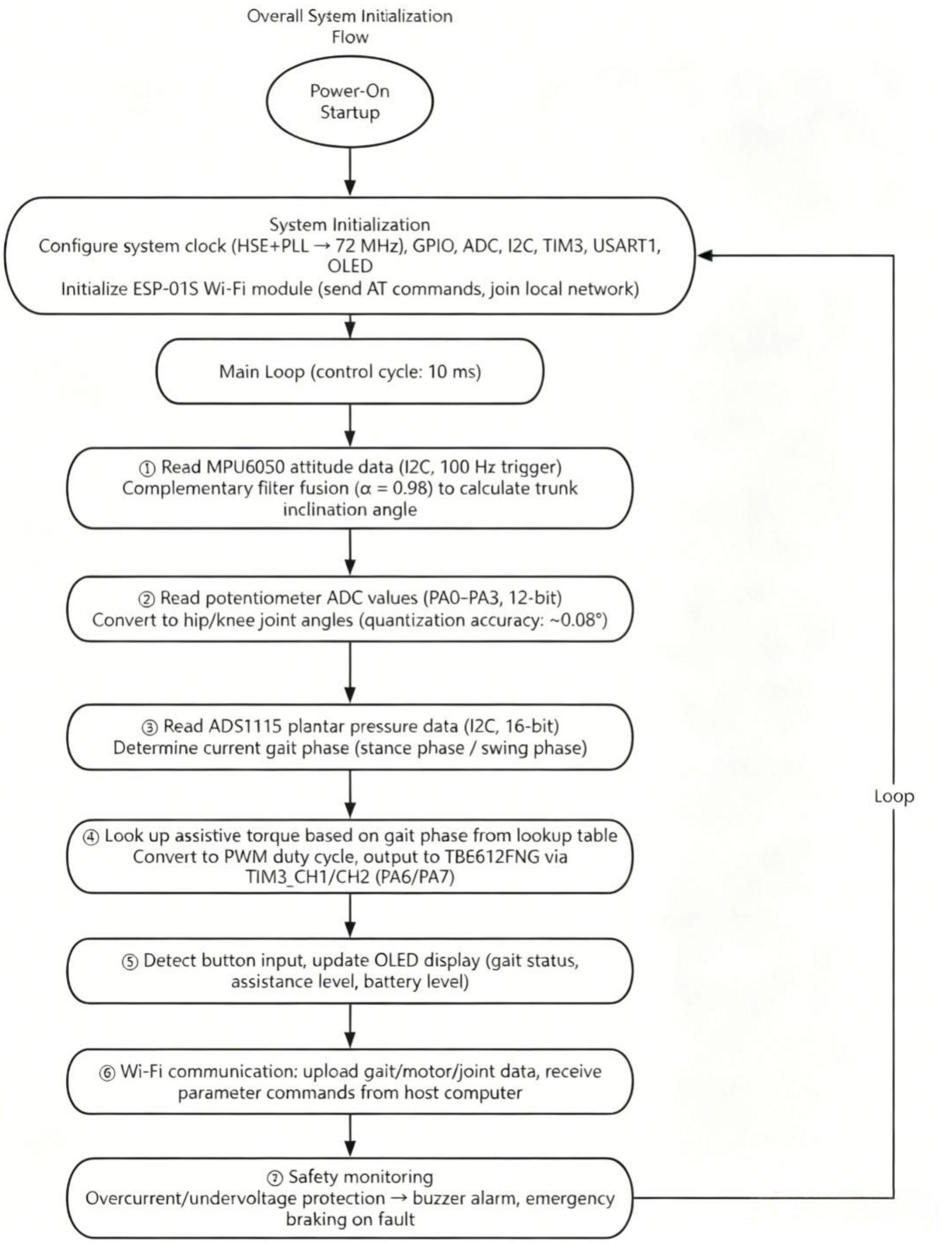

Figure 6. System operation flowchart.

4.2. Host Computer Software Design

The host computer software is developed using Python 3.10 and PyQt5, connecting to the STM32 main controller via Wi-Fi (ESP-01S) through TCP Socket to receive sensor data such as gait phase, joint angles, plantar pressure, and motor current in real time. The main interface is divided into four functional areas:

(1) Real-time data monitoring area — displaying gait waveforms, motor current bar charts, plantar pressure heatmaps, and battery information;

(2) Parameter configuration area — providing adjustments for assistance level, walking mode, speed gear, and motor setting, with commands sent to the main controller via TCP;

(3) Intelligent function module area — integrating obstacle detection and warning, assistance curve playback, and historical data query;

(4) Data storage module — sensor data is archived in CSV format and simultaneously stored in an SQLite database, supporting the export of test reports. The communication status bar displays Wi-Fi connection status in real time. The host computer design flow is shown in Figure 7, and the UI interface is shown in Figure 8.

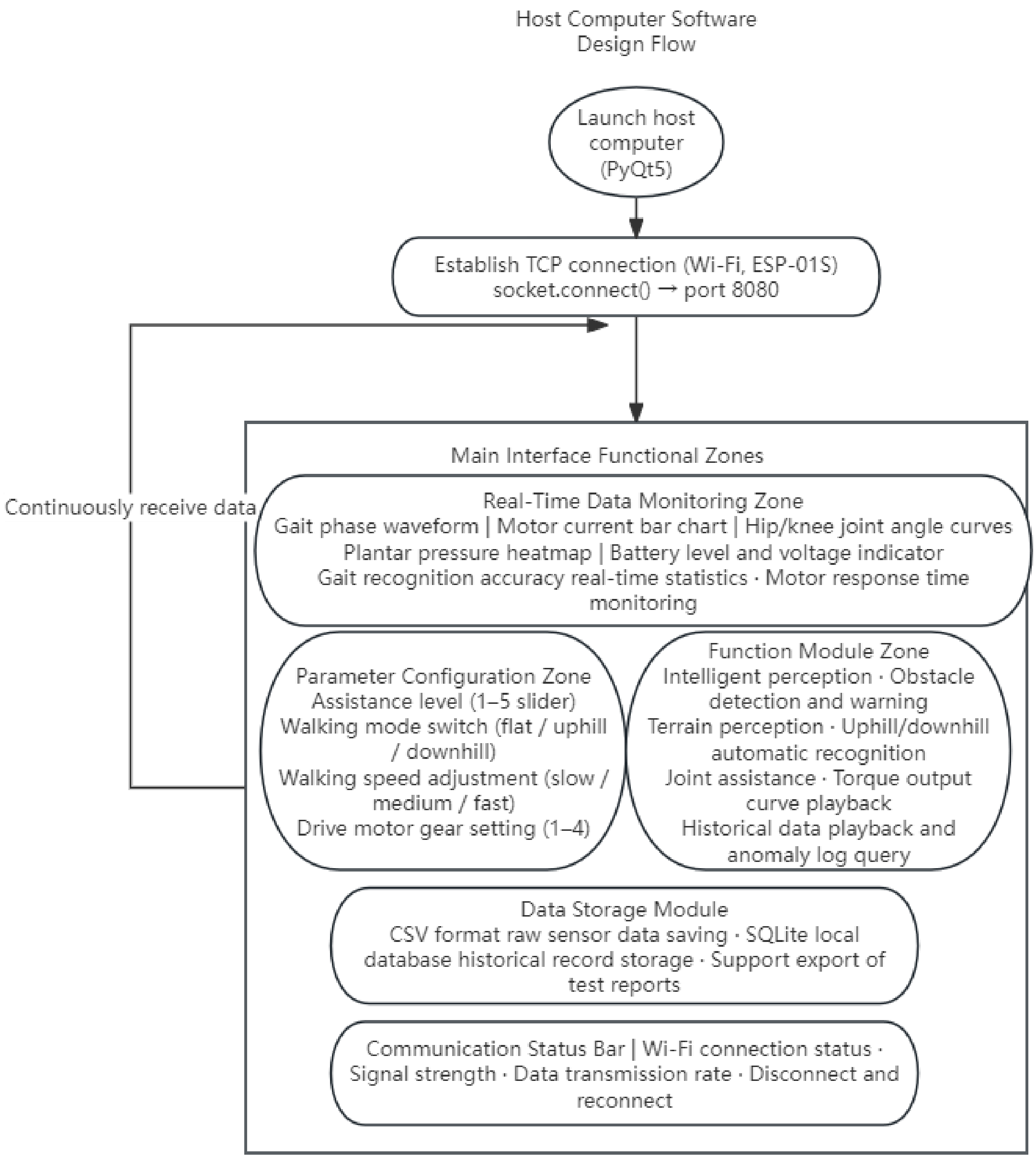

Figure 7. Host computer software design flowchart.

Figure 8. Host computer UI interface.

5. Experimental Results

To thoroughly verify the actual performance of the designed control system, a series of systematic tests were meticulously conducted in a controlled laboratory environment. These tests included assessments of sensor accuracy, evaluations of gait recognition accuracy, measurements of motor assistance response times, and analyses of overall power consumption. The comprehensive test results are presented in Table 2 for further examination.

The test results indicate that all system performance indicators successfully meet the established design requirements. Notably, the joint angle sensing accuracy and plantar pressure resolution have both reached the expected levels, providing highly reliable input data for the gait algorithm. The gait phase recognition accuracy of 93.6% not only meets practical requirements but also demonstrates robust performance, with a small number of misrecognitions occurring primarily during the critical moments of phase transition. Additionally, the motor assistance response time of just 22 ms is well below the human perception threshold (approximately 50 ms), ensuring a natural and intuitive feel to the assistance provided. Furthermore, the overall battery life, lasting approximately 1.3 hours, adequately meets the basic mobility needs of elderly users during daily activities. Looking ahead, future improvements can be achieved by optimizing motor drive strategies and upgrading to higher-capacity batteries, which would significantly enhance and extend operating time for better user experience.

Table 2. Test results.

Test Item	Test Result	Test Method	Specification Requirement
Joint Angle Accuracy	Mean error ±1.3°	Comparison with optical goniometer (30 samples)	≤ ±3°
Plantar Pressure Resolution	Pressure resolution 0.5 N	Weight calibration (0–50 N, step 5 N)	≤ 1 N
Gait Phase Recognition Rate	Accuracy 93.6%	10 healthy subjects, 5 min walking each, manually annotated for comparison	≥ 90%
Motor Assistance Response Time	Mean response time 22 ms	Oscilloscope measurement from PWM command to motor speed stabilization	≤ 30 ms
Overall Power Consumption	Mean power 18.4 W, battery life ~1.3 h	Ammeter measurement under full-speed operation	Battery life ≥ 1 h

6. Conclusion

This paper presents the design and implementation of a wearable lower-limb assisted walking device control system based on the STM32F103C8T6 microcontroller. The system adopts a modular design approach, achieving multi-dimensional gait information acquisition through MPU6050 inertial sensors, rotary potentiometers, and plantar pressure sensors. After fusion processing using a complementary filter algorithm, gait phases are identified. The TB6612FNG drivers control four DC motors to output joint assistive torque, with the PWM duty cycle adjusted in real time according to the gait phase. The ESP-01S Wi-Fi module enables wireless communication with the host computer, supporting real-time data monitoring and remote parameter configuration. The OLED display, buttons, and buzzer provide a local human-machine interaction interface.

Experimental results demonstrate that the system achieves a gait phase recognition accuracy of 93.6%, motor assistance response time of 22 ms, joint angle acquisition error of ±1.3°, and overall battery life of approximately 1.3 hours. All performance indicators meet the design requirements, and the system can effectively provide lower-limb walking assistance support for the elderly. Future research directions include: introducing adaptive assistance algorithms to accommodate gait variations among different users, improving gait recognition accuracy based on machine learning, optimizing motor control strategies to enhance energy efficiency, and conducting clinical rehabilitation application evaluations to further validate the practical value of the system.

Acknowledgements

The authors would like to express their gratitude to the Department of Intelligent Manufacturing Engineering, University of Electronic Science and Technology of China, Chengdu Campus, for providing experimental equipment and technical support.

References

[1] Xu, Y. F., Zhang, H., Yu, L. F., et al. (2023). Study on the structure and control of intelligent training walker. *Mechanical & Electrical Engineering Technology*, 52(12), 86–91.

[2] Tan, J. L. (2024). Design analysis and experimental research on lower-limb assistive exoskeleton [Master's thesis]. *Hefei University of Technology*, Hefei.

[3] Zeng, T. J. (2025). Design and implementation of a two-degree-of-freedom hip joint exoskeleton mechanism for elderly walking assistance [Master's thesis]. *University of Electronic Science and Technology of China*, Chengdu.

[4] Li, J. F., Zhao, P. B., Zhang, L. Y., et al. (2022). Research progress on wearable lower limb exoskeleton rehabilitation robots. *Robot*, 44(5), 618–632.

[5] Sun, X. Q., & Yu, X. D. (2024). Review of gait recognition systems for lower limb exoskeleton robots. *Journal of Electronic Measurement and Instrumentation*, 47(1), 1–10.

[6] Qian, Z. X., Xing, W., Bu, C. G., et al. (2024). Gait phase recognition of lower limb exoskeleton rehabilitation robot. *Information and Control*, 53(3), 289–298.

[7] Han, Y. L., & Wang, X. S. (2022). Dynamics modeling and simulation analysis of lower limb assistive exoskeleton. *Mechanical Science and Technology for Aerospace Engineering*, 41(9), 1328–1335.

[8] Liu, H. L., & Yang, S. (2022). STM32 library development practical guide (3rd ed.). *China Machine Press*, Beijing.

[9] Liang, Y. L., Zhang, M. L., Zhang, X. J., et al. (2023). Gait phase recognition of lower limb exoskeleton based on force sensing and IMU. *Chinese Journal of Scientific Instrument*, 44(6), 156–165.

[10] Wu, Q. C., & Wang, X. S. (2023). Assistive control method for soft lower limb exoskeleton based on multi-source information fusion. *Journal of Mechanical Engineering*, 59(17), 175–186.

[11] Chen, X. H., & Zhao, Y. S. (2023). Design of human-machine interaction control system for wearable lower limb exoskeleton. *Application of Electronic Technique*, 49(8), 92–97.

[12] Wang, Y., Liu, Z. S., & Ge, Y. J. (2022). Kinematic analysis of human lower limbs and structural design of exoskeleton. *China Mechanical Engineering*, 33(15), 1824–1832.

[13] Zhou, G. Q., & Zhang, J. W. (2023). WiFi wireless data acquisition and remote monitoring system based on ESP8266. *Automation and Instrumentation*, 38(5), 62–67.

[14] Zhang, J. X., Cao, S. S., Yang, X. F., et al. (2022). Analysis of gait stability and lower limb kinematic characteristics in the elderly. *Journal of Medical Biomechanics*, 37(6),

1045–1051.

[15] Huang, J. P., & Wang, F. (2023). Design of low-power power management system for wearable devices based on STM32. *Chinese Journal of Power Sources*, 47(3), 412–417.